(Pyridyl)-Aminotriazoles as Versatile Synthetic Synthons: Amido Complexes, "Normal" Triazole-Based Imines and Metallo Mesoionic Imines

Richard Rudolf, Biprajit Sarkar*

Institut für Anorganische Chemie, Universität Stuttgart, Pfaffenwaldring 55, 70569 Stuttgart, biprajit.sarkar@iac.uni-stuttgart.de

KEYWORDS mesoionic imines, metallo mesoionic imines, electronically adaptive compounds, C-F activation, C-H activation.

ABSTRACT: Mesoionic compounds are currently hugely popular in several fields such as organic chemistry, organometallic chemistry and homogeneous catalysis. A new class of mesoionic compounds are the mesoionic imines (MIIs). For MIIs based on a 1,2,3-triazole core, the synthetic strategy involves alkylation/arylation of the triazole-*N*3 atom and subsequent deprotonation to deliver MIIs. We present here 5-amino-4-pyridyl-1,2,3-triazole as an alternative and versatile synthon for generating metallo-MIIs. In this approach, we make use of metallation at the N-pyridyl/*N*3-traizole chelating pocket (instead of quarternisation of *N*3-triazole) and subsequent deprotonation to generate highly versatile and tunable metallo-MIIs. These unprecedented metallo-MIIs contain a highly nucleophilic N-donor site, and a tunable electrophilic metal site within the same platform. Apart from displaying strong and directed H-bonding interactions like their "classical" MII analogues, the metallo-MIIs engage in aromatic C-F activation as well as *meta*-C-H activation reactions. Facile synthesis of homo and heterodincuelar complexes which contain a mixed coordinative saturation/unsaturation with these metallo-MICs is presented. Apart from the metallo-MICs we have also used 5-amino-4-pyridyl-1,2,3-triazole as a viable precursor to generate the first examples of amido-1,2,3-triazole complexes and the first example of a "normal" (and not mesoionic) 1,2,3-triazole based imine. Apart from a combination of synthetic chemistry, multinuclear NMR spectroscopy and single crystal X-ray diffraction, (TD)DFT calculations were also used to shed light on the electronic structure and the frontier orbital situation of these compounds. Our results thus establish metallo-MIIs as a versatile new class of mesoionic compounds that combine the modularity of click reactions, with the functionality of metal fragments to generate electronically ambivalent compounds with a huge potential in synthetic chemistry, catalysis and beyond.

Polypyridines are an extremely important class of ligands in coordination chemistry. The strong π-accepting properties of these ligands make them special, with 2,2´-bipyridine (bpy, Chart 1) arguably being the most prominent class of polypyridine ligands. Metal complexes of such ligands have found use, amongst others, in electrocatalysis[1–12], photocatalysis[13–22], spin-crossover materials[23–28] and homogenous catalysis[29–36] besides applications in medicinal chemistry[37]. N-heterocyclic carbenes (NHCs, Chart 1) on the other hand are usually considered strongly σ-donating ligands, and they are now ubiquitous in organometallic chemistry and homogeneous catalysis.[38–44] A relatively new twist in the broad NHC field has been the emergence of the so-called mesoionic carbenes (MICs, Chart 1).[45–47] In particular, the 1,2,3-triazolylidene type MICs offer unprecedented ligand tuning possibilities[48,49] because of their modular synthesis through the Nobel prize winning "Click" chemistry.[50–56]

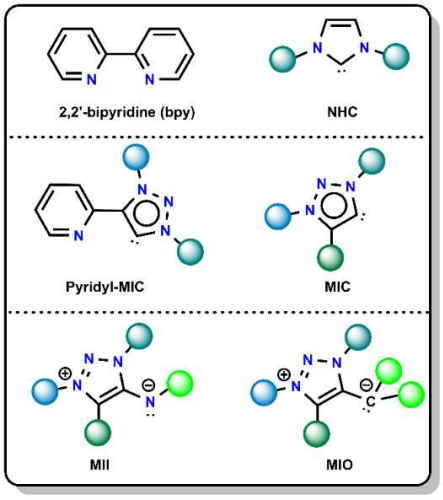

Chart 1. Structural comparison of selected, reported ligand frames discussed herein.

In this context, the pyridyl-MIC ligands have emerged as a privileged ligand that combines the strongly σ-donating properties of MICs with the π-accepting properties of pyridine.[49,57–69] Metal complexes of pyridyl-MICs have been shown to stabilize

an oxidized chromiumtetracarbonyl-complex[63] and intermediates postulated in the electrochemical reduction of protons with a RhCp*-complex bearing a pyridyl-MIC ligand[70]. Newer additions to mesoionic compounds based on a 1,2,3-triazole core include mesoionic olefins (MIOs, Chart 1) and mesoionic imines (MIIs, Chart 1). Both compound classes have already found use in the stabilisation of elusive fragments[71,72], as organocatalysts[73–76], as chromophores[77,78] and as ligands in main-group element chemistry[78,79] and transition metal complexes[78–80].

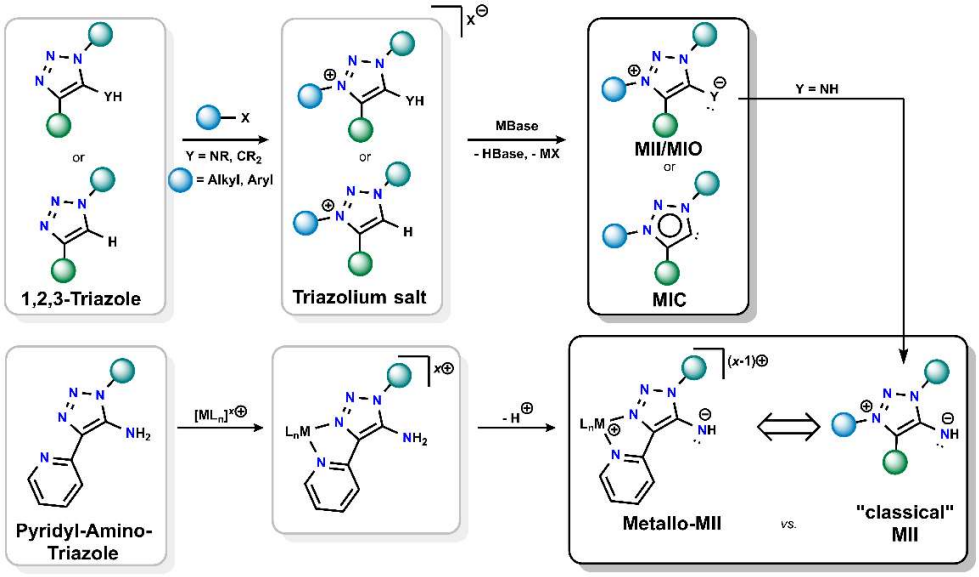

Scheme 1. Conceptual comparison of the synthesis of "classical" MICs/MIIs/MIOs with Metallo-MIIs.

One common feature in the synthesis of triazole-containing MICs, MIOs and MIIs is the formation of a triazole-core through one type of cycloaddition reaction, the subsequent alkylation (or arylation) of the N3-triazole atom, and eventual deprotonation to deliver the aforementioned intriguing compounds (Scheme 1).[45,75,76,78,79,81] Having recently developed a facile synthetic route for MIIs[79,80], and having also shown that pyridyl-MICs are a special compound class in organometallic chemistry and catalysis, we have now turned our attention to (pyridyl)aminotriazoles (Scheme 2-4 and 6). In particular, we address three different question related to (pyridyl)aminotriazoles in this work: a) Are pyridyl substituted amido-triazole ligands accessible? b) Is preferential methylation at the *N*2-nitrogen (and not *N*3) atom of 1,2,3-triazoles possible in order to generate "normal" (and not mesoionic) triazole-based imines? c) Can metal chelation at the pyridyl-N/triazole-*N*3 be a viable alternative to the *N*3-alkylation/arylation route for the generation of metallo MIIs? In particular, the latter point, if successfully executed, would open up a completely new accessibility to MIIs with properties that would not be possible with the alkytion/arylation strategy. This is because metal fragments are able to offer different types of functionality (e.g. redox states, different charges, spin states, photoactivity, coordination ambivalence) which is not possible if simple "innocent" fragments like alkyls or aryls are used for the quarternisation of the *N*3-atom of the 1,2,3-triazole ring. In the following, we present results from synthetic chemistry, reactivity studies, and quantum chemical calculations to address each of the three points mentioned above. We also show first results in which the metallo MIIs have been used either for C-F activation reactions or for the selective meta-C-H activation of aromatic rings.

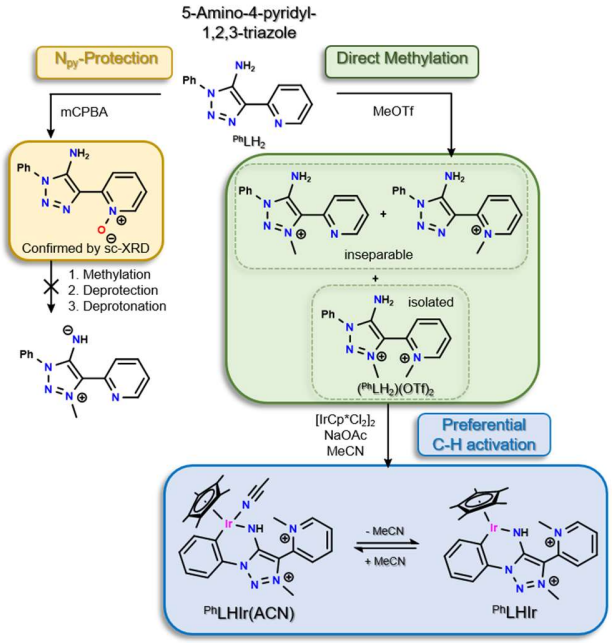

Scheme 2. Representation of previous work on Py-substituted 5-amino-triazoles $^{Ph}LH_2$ and MIIs.[79]

Treatment of the triazole **LH_2** with $Zn(HMDS)_2$ in toluene selectively yielded the homoleptic complex **$[LH]_2Zn$** in quantitative yields. The Zn-complex is a moisture and air sensitive solid (Scheme 3). To best of our knowledge, **$[LH]_2Zn$** represents the first 5-amido-1,2,3-triazole complex reported.

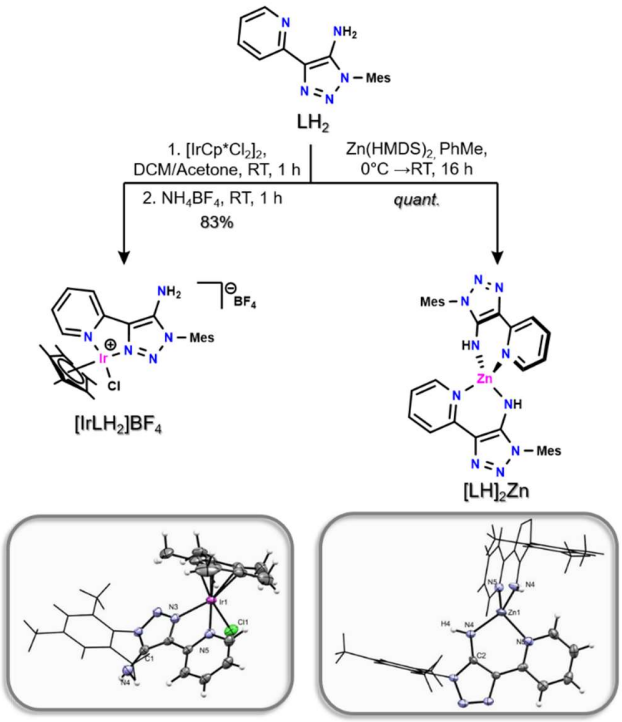

Scheme 3. Synthesis of $[IrLH_2]BF_4$ and $[LH]_2Zn$ and the respective molecular structures in ORTEP-representation in the crystals obtained by single-crystal XRD (right). Ellipsoids are set to 50% probability. Selected fragments are displayed in wireframe-representation for clarity. Counter-anions, if present, are omitted for clarity.

Direct methylation of **$[LH]_2Zn$** to **$[LH_2]X$** with either Me_3OBF_4 or MeOTf yielded crude reaction mixture from which no product could be further isolated or characterized (Scheme 4). We therefore conducted transmetalation reactions of **$[LH]_2Zn$** with $[IrCp^*Cl_2]_2$ either in the presence or absence of a methylating agent to further gauge the reactivity of **$[LH]_2Zn$**. By transmetalation in absence of methylating agent, the formal amide-bound Ir-complex **[LHIr]** could be isolated in a low yield of 34% (Scheme 4). From examinations of the crude mixture *via* ^{1}H-NMR-spectroscopy we identified a second product from the reaction which can be assigned to **$[IrNH_2]Cl$** (Supporting Information Fig. S22). Unfortunately, besides **[LHIr]** we were not able to isolate **$[IrNH_2]Cl$** from the crude material. **$[IrNH_2]^+$** as the **BF_4^-** salt can be selectively synthesized by the reaction of **LH_2** with $[IrCp^*Cl_2]_2$ over the course of two hours (Scheme 3). **$[IrNH_2]BF_4$** was obtained after anion exchange in good yields of 83% and characterized by NMR-, UV-Vis-spectroscopy (see below, Figure 2 b)) and single-crystal XRD (Scheme 3).

Methylation of **$[LH]_2Zn$** with Me_3OBF_4 followed by the addition of $[IrCp^*Cl_2]_2$ yielded a mixture of two compounds which were identified by ^{1}H-NMR-spectroscopy (Supporting Information Fig. S23): One of both being **$[IrLH_2]BF_4$**. Single-crystals obtained from the crude mixture by overlayering a DCM-solution of the crude with Et_2O were subjected to X-ray diffractometry (Scheme 4). The structure obtained thereof unveiled the second component of the reaction to be **$[L'HIr]BF_4$** *via* methylation of the *N*2-atom of the triazole-moiety not the *N*3-atom as expected. By formulation of resonance structures **$[L'HIr]BF_4$** can be identified as an iridium-complex with a non-mesoionic imine-ligand (Scheme 4). This is the first example of a metal complex with a "normal" 1,2,3-triazole-based MII. Reaction of **$[LH]_2Zn$** with MeOTf followed by transmetalation with $[IrCp^*Cl_2]_2$ resulted in a quantitative conversion to the N_{Py}-N_{Trz}-coordinated product **$[IrLH_2]OTf$** according to the ^{1}H-NMR-spectrum obtained from the crude mixture (Scheme 4, Supporting Information Fig. S24). In order to transform **$[LH]_2Zn$** to **[IrLH2]X** (X = BF_4, Cl, OTf), formally a proton has to be added. This opens up the question of the origin of the proton source. Examination of the methylating agents Me_3OBF_4 and MeOTf by ^{1}H-NMR-spectroscopy suggested minor acidic contaminations of the used MeOTf while Me_3OBF_4 as obtained by the supplier is sufficiently pure. We therefore assume that the quantitative conversion of **$[LH]_2Zn$** to **$[IrLH_2]OTf$** under the presence of MeOTf might be the result of catalytic amounts of acidic contamination. It was already pointed out by Timothy and co-workers[82] that the cationic N_{Py}-N_{Trz}-coordination to Ir(III)-centers is preferred over the formal triazolide-coordination mode thus backing up the hypothesis stated before.

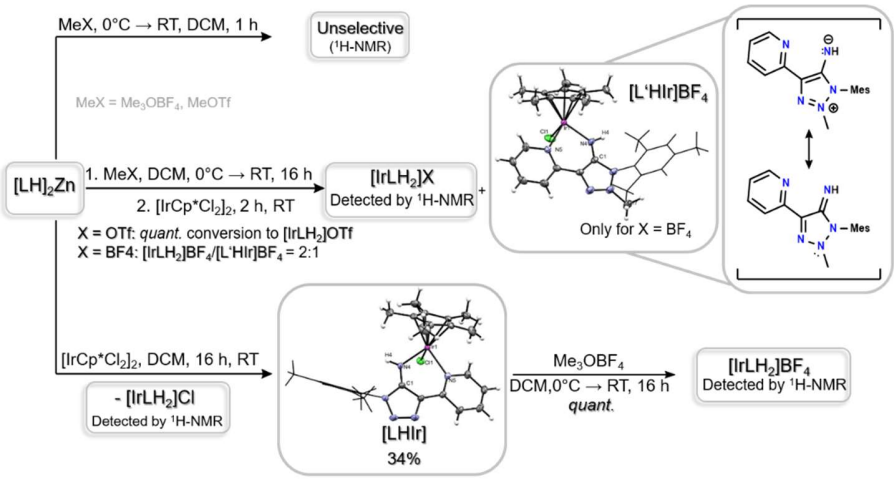

Scheme 4. Reactivity of $[LH]_2Zn$ towards methylation and transmetalation with $[IrCp^*Cl_2]_2$ and the respective molecular structures in ORTEP-representation in the crystals obtained by single-crystal XRD. Ellipsoids are set to 50% probability. Selected fragments are displayed in wireframe-representation for clarity. Counter-anions, if present, are omitted for clarity

As observed previously by us with the corresponding phenyl-substituted derivative (Scheme 2)[79], the reaction of **LH_2** with methylating agents like MeOTf or Me_3OBF_4 yielded a crude mixture of the possible monomethylated products or the bis-methylated product **$[LH_2]X_2$** from which only the latter could be isolated in the case of X = BF_4 (Scheme 5). Compared to the *N*1-phenyl substituted derivative (**$^{Ph}LH_2(OTF)_2$**[79]), the corresponding *N*1-site of **$[LH_2]X_2$** contains a mesityl-subtituent and is therefore blocked for aromatic C-H activation. To further analyse the behavior towards C-H activation, **$[LH_2]X_2$** was reacted under basic conditions with $[IrCp^*Cl_2]_2$. According to the ^{1}H-NMR-spectrum of the crude reaction mixture the desired IrCp*-complex with a bidentate MII-ligand **$[LHIr](BF_4)_2$** via C-H-activation of the *ortho*-H on the Py-site was formed during this reaction as evident by three distinct multiplets in the aromatic region beside the singlet assigned to the aromatic Mes-*H* protons (Scheme 5).

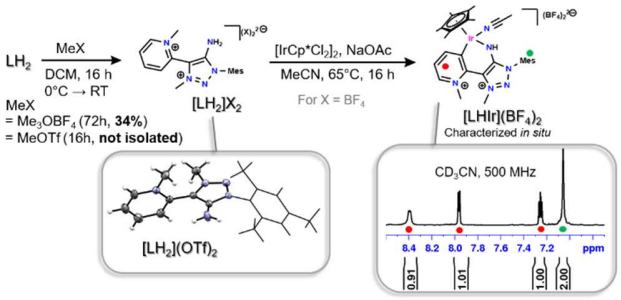

Scheme 5. Methylation of LH_2 and subsequent C-H activation with $[IrCp^*Cl_2]$. For $[LH_2](OTf)_2$ the molecular structure elucidated by sc-XRD is shown in ORTEP-representation. Ellipsoids are set to 50% probability and selected fragments are displayed in wireframe representations for clarity. Counter-anions are omitted for clarity. For $[LHIr](BF_4)_2$ a cut-out of the corresponding ^{1}H-NMR-spectrum (crude product) is shown and peaks are assigned to the structure thereof.

The coordination of an auxiliary MeCN-ligand as seen in the proposed structure of **$[LHIr](BF_4)_2$** (Scheme 5) can be deduced from the red color of the thus obtained product, the relatively high-field shifted signal assigned to the N*H*-proton (δ = 3.94 ppm) and a signal with a relative integral of three with a chemical shift (δ = 1.96 ppm) expected for coordinated MeCN. This compound is the first example of a metal complex that is simultaneously coordinated by a remote carbene and a MII donor. The product decomposes over the course of several hours even under inert conditions thus making a further characterization or isolation impossible.

$[IrNH_2]BF_4$ can be considered a viable precursor for MII (Scheme 1) with an IrCp*-moiety in the backbone. In this context, **$[IrNH_2]BF_4$** was employed in deprotonation and metalation reactions known for classical MIIs.[79]

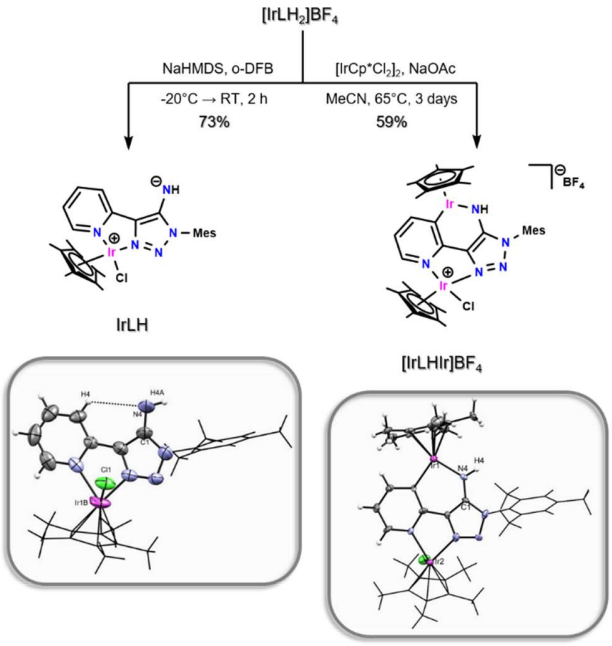

Scheme 6. Reactivity of the triazolium salt $[IrLH_2]BF_4$ towards deprotonation and C-H-activation with $IrCp^*Cl_2$with the corresponding molecular structures elucidated by sc-XRD displayed in ORTEP-representation. Ellipsoids are set to 50% probability and selected fragments are displayed in wireframe representations for clarity.

Counter-anions, if present, are omitted for clarity. *o*-DFB: *ortho*-difluorobenze.

Deprotonation of **[IrLH$_2$]BF$_4$** under typical conditions with NaHMDS in o-DFB yielded the corresponding metallo-MII **IrLH** as a bright-orange powder (Scheme 6). The product identity was confirmed by NMR-spectroscopy, sc-XRD and CHN-analysis. With a length of 1.301(5) Å (Table 1), the C1-N4 bond in **IrLH** is in the same range as observed for classical MIIs (such as ^{R}**L** (R = Mes[79], Fc[80], Ph[79]), Figure 1) and therefore best characterized as a C-N bond with significant double bond character. Like ^{R}**L**, **IrLH** shows intramolecular H-bonding with the adjacent *o*-proton of the flanking substituent in solid state (XRD-structure on the left in Scheme 6). **IrLH** is an air- and moisture sensitive compound and decomposes in the presence of CH_2Cl_2 or MeCN. This observation contrasts the reactivity of "classical", purely organic MIIs, which can be dissolved in non-dried, aprotic solvent and CH_2Cl_2/MeCN respectively without undergoing hydrolysis or further reactions. Reaction of **IrLH** with $[Rh(CO)_2Cl]_2$ in THF overnight at room temperature afforded a mixture of two compounds from which the desired Rh-complex **IrLHRh** could be identified via ^{1}H-NMR-, IR-spectroscopy and sc-XRD (Scheme 7). Although the nature of the side-product remains unclear, it was possible to separate **IrLHRh** from the mixture by extraction with toluene.

The CO-stretching modes of **IrLHRh** were examined *via* FTIR-spectroscopy from which a TEP[83] (Tolmann electronic parameter) of 2045 cm^{-1} was determined. Contrary to the observation of **IrLH** being a) a stronger base (hydrolysis under ambient conditions) and b) a stronger nucleophile (reaction with MeCN and DCM) compared to classical MIIs (like ^{Mes}**L**[79], Figure 1), the obtained TEP suggests that **IrLH** is a slightly weaker net-electron donor as ^{Mes}**L**. As the TEP-value combines effects of donating and accepting properties which influence the TEP-value in a contrary fashion, the observed reactivity of **IrLH** might be the result of higher π-accepting contributions in **IrLH**. In earlier reports, we have pointed out that MIIs might be able to engage in π-backbonding.[79,80] To gain further insight, theoretical calculations were conducted (Figure 1).

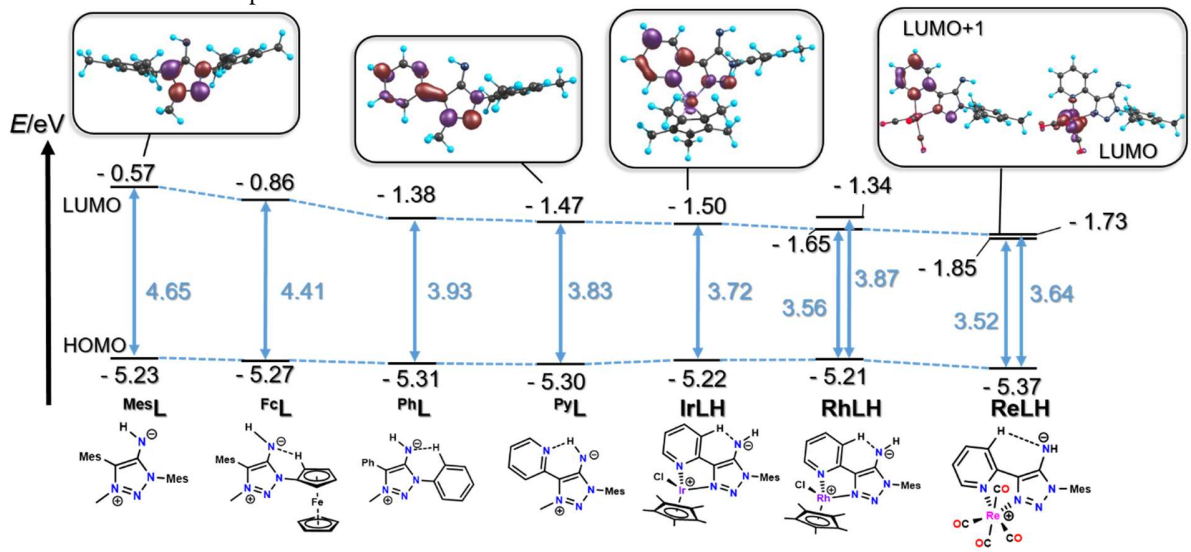

Figure 1. Molecular frontier orbitals of selected MIIs and the respective energies and HOMO-LUMO-energy gap. Isovalue = 0.0622. References: ^{Mes}**L** and ^{Ph}**L** [79]. ^{Fc}**L**[80]. ^{Py}**L**, **RhLH** and **ReLH**: Hypothetical molecules whose structures were deduced from molecular structure elucidated by single-crystal XRD of similar compounds and then subjected to geometry optimization. Only selected orbitals are displayed to highlight the changes of the electronic structure by different substitutions in order to remain clarity of the figure. Level of theory: PBE0/def2-TZVP/SARC-ZORA-TZVP(Ir, Re, Rh)/CPCM(CH_2Cl_2). Computational details can be found in the SI.

The frontier MOs (Figure 1) of the differently decorated MIIs qualitatively show the same characteristics: The HOMO-orbital mostly resides on the very electron rich N_{exo}. This observation is in line with reactivity studies, which show that MIIs act as strong N-donors (Scheme 7).[79,80] The LUMO of MIIs mostly resides on the triazole-backbone with π^*-symmetry – an observation which lead us to discuss possible accepting properties of MIIs in previous reports.[79,80] The flanking-substituents on the triazole-backbone can heavily influence the degree of delocalization and therefore the LUMO-energy. By parallelization of the flanking substituent with the triazole-ring (e.g. through H-bonding as present in MIIs) the degree of conjugation of the system increases and thus the respective LUMOs are energetically lowered. This leads presumably to a more accessible back-donation from the metal to the MII-ligand. In the case of the metallo-MII **IrLH** and the theoretically calculated Py-substituted MII ^{Py}**L** this effect is quite pronounced compared to the bismesityl-substituted derivative ^{Mes}**L**. Therefore, it is reasonable to assume, that the higher TEP-value of **IrLH** compared to ^{Mes}**L** is the result of a higher π-acidity of **IrLH** thus giving unprecedented experimental proofs for MIIs to act as acceptor-ligands.

The high donating-capacities of **IrLH** were tested in the C-F activation reaction of hexafluorobenzene (Scheme 7). The reaction leads to the condensation of C_6F_6 with the metallo-MII **IrLH** under the formation of the C_6F_5-MII **IrLC$_6$F$_5$** and formal depletion of HF according to sc-XRD of single-crystals obtained from the reaction mixture in deuterated THF (Scheme 7).

Further analysis of the reaction mixture *via* ^{1}H- and ^{19}F-NMR-spectroscopy implies the formation of a side product. Presumably, the C_6F_5-substituted triazolium salt **[IrLH(C_6F_5)]F** is formed after nucleophilic aromatic substitution of C_6F_6, which protonates another **IrLH**-molecule (**IrLC$_6$F$_5$** is a weaker base than **IrLH** due to the electron-withdrawing C_6F_5-substituent) yielding **IrLC$_6$F$_5$** and the corresponding triazolium salt **[IrLH$_2$]X** (X = F, HF_2).[84–87] As the solubility of **IrLC$_6$F$_5$** and **[IrLH$_2$]X** is very similar, we were not able to separate both compounds (Scheme 7).

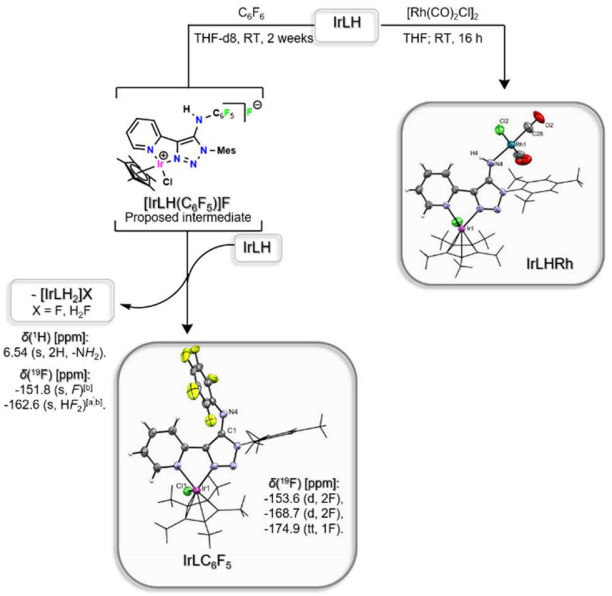

Scheme 7. Reactivity of the metallo-MII IrLH towards C_6F_6 and $[Rh(CO)_2Cl]_2$ with the respective molecular structures in ORTEP-representation in the crystals obtained by single-crystal XRD. Ellipsoids are set to 50% probability. Proposed mechanism for the formation of IrLC$_6$F$_5$ and [IrLH$_2$]X based on the experimentally determined chemicals shifts . X = F, H2F. [a]: ref. [86,87]. [b]: ref. [84]

Reaction of **[IrLH$_2$]BF$_4$** with $[IrCp^*Cl_2]_2$ under basic conditions (NaOAc) yielded the dinuclear Ir-complex **[IrLHIr]BF$_4$** via C-H activation at the *meta* position on the Py-substituent (Scheme 6). Spectroscopic (NMR, UV-Vis (see below, Figure 2 b) and Supporting Information Fig. S49 and S51)) and crystallographic methods elucidated the product composition and connectivity within the molecule. From the dark-green color and the downfield shifted signal assigned to the N*H*-Ir moiety in the ^{1}H-NMR-spectrum (Supporting Information Fig. S32 and S34) it was apparent that a coordinatively unsaturated Ir-complex was formed during the reaction. The metallo-MIIs can thus be used for facile *meta*-C-H activation and the formed dinuclear complex is also a rare example in which a coordinatively saturated and a coordinatively unsaturated iridium center are part of the same molecule. The coordinative unsaturation was further proven by reactivity studies: The addition of Ph_3P to **[IrLHIr]BF$_4$** resulted in an immediate change in color from dark-green to yellow accompanied by the formation of two new species according to the ^{1}H- and ^{31}P-NMR-spectra (Supporting Information Fig. S36 and S38) of the reaction mixture. In the ^{1}H-NMR-spectrum the signal assigned to the N*H*-moiety is significantly shifted towards a higher field (9 ppm *vs.* 1 ppm) while a new resonance in the ^{31}P-NMR-spectrum at 9.1 ppm provides strong indications for the formation of **[IrLHIrPPh$_3$]BF$_4$** (Scheme 8).[80] Sc-XRD of single-crystals obtained from the reaction mixture proved the coordination of the phosphine-ligand onto the free coordination site. The appearance of signals in a set of two in both the ^{1}H- and ^{31}P-NMR-spectra of **[IrLHIrPPh$_3$]BF$_4$** allows for speculation of possible (side)-products. As **[IrLHIrPPh$_3$]BF$_4$** was obtained as a reasonably pure compound according to CHN-analysis, we assume that a diastereomeric mixture was obtained. The phosphine-ligand can attack the Ir-atom either on the Cp*- or Cl-face forming either the Cp*-Cp*-trans or Cp*-Cp*-cis diastereomer. The molecular structure of the cis-diastereomer could be elucidated by sc-XRD (Scheme 8).

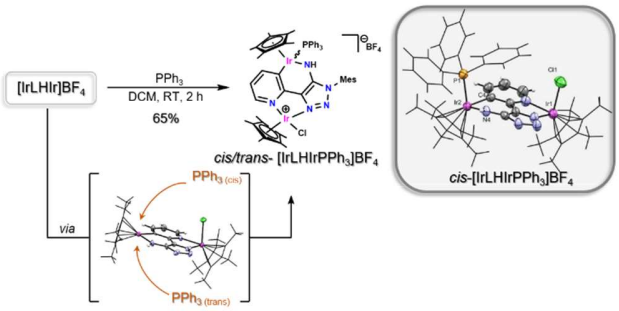

Scheme 8. Reaction of the coordinatively unsaturated bimetallic Ir-complex [IrLHIr]BF$_4$ towards PPh_3 with the respective molecular structures in ORTEP-representation in the crystals obtained by single-crystal XRD (right). Selected fragments are displayed in wireframe representation. Counter-anions are omitted for clarity.

Interestingly, the complex **[IrLHIr]BF$_4$** is stable under ambient conditions and MeCN will not coordinate unlike observed for the readily decomposing derivative **[LHIr](BF$_4$)$_2$** (Scheme 5) and the previously reported dicationic complex **^{Ph}LIr(ACN)/^{Ph}LIr** (Scheme 2).[79] This might be the result of two effects: Compared to **[LHIr](BF$_4$)$_2$** (with a neutral MII-ligand), **[IrLHIr]BF$_4$** bears a monoanionic MII-ligand frame thus providing more stabilization through stronger electron-donation.[80] On the other hand further electron density in **[IrLHIr]BF$_4$** is shared from the IrCp*Cl-fragment through the Py-ligand into the IrCp*-fragment by π-donation as evident from the crystallographic data (Figure 2a)). The N_{Py}-Ir bond from **[IrLH$_2$]BF$_4$** to **[IrLHIr]BF$_4$** is shortened, while the corresponding N_{Trz}-Ir bond is elongated after coordination to the second IrCp*-moiety. After coordination of the phosphine-ligand (**[IrLHIrPPh$_3$]BF$_4$**) to the free coordination site of **[IrLHIr]BF$_4$** this effect is reversed as evident by an elongated N_{Py}-Ir and shortened N_{Trz}-Ir while the C_{Py}-Ir bond is elongated in that row. Thus, the Py-ligand can act as a mediator of electron density and stabilize the unsaturation on the Ir-atom.

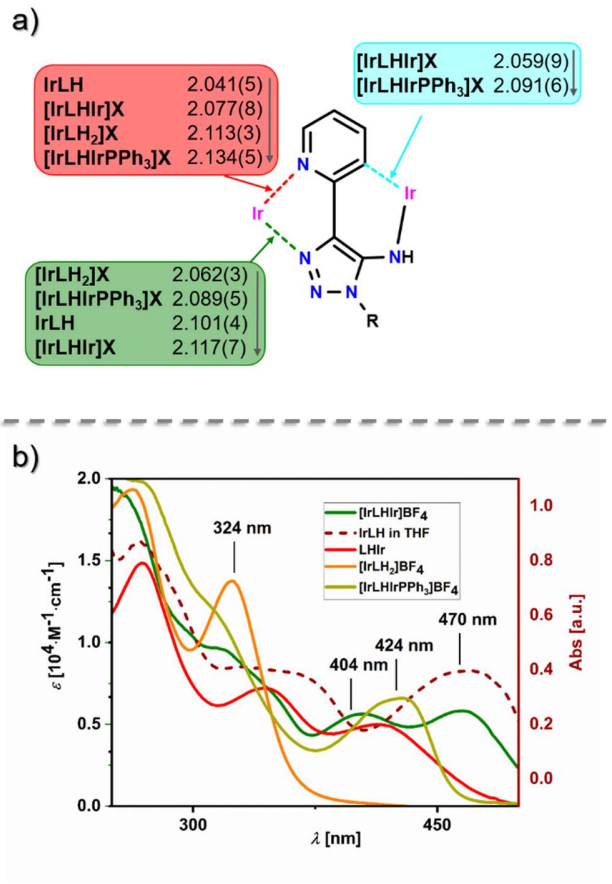

Figure 2. a) Representation of relevant bond length (in Å) deduced from sc-XRD data for selected compounds. b) UV-Vis spectra of selected compounds measured in CH_2Cl_2. The UV-Vis spectrum of **IrLH** was measured in THF due to reaction of the substrate with CH_2Cl_2. The supporting TD-DFT calculations suggest no solvent effect on the qualitative shape of the UV-Vis spectra. For **IrLH** no quantitative analysis *via* Lambert-Beer's-Law was conducted due to concentration dependent agglomeration of MIIs in solution. Therefore, a single UV-Vis at a fixed concentration is displayed.

The electronic structure of some selected Ir-complexes was further analyzed *via* UV-Vis spectroscopy (Figure 2 b)) and supported by (TD)-DFT calculations (see SIs for computational details). Except for the dinuclear complexes **[IrLHIr]BF$_4$** and **[IrLHIrPPh$_3$]BF$_4$**, the transition in the VIS-region of the spectrum mostly translates to LLCT from N_{exo} onto the Py-substituent and LMCT from N_{exo} to the Ir-atom. The absorption at lowest energy for the triazolium salt **[IrLH$_2$]BF$_4$** at 324 nm red-shifts upon deprotonation to **IrLH** to 470 nm which can be explained by a lower HOMO-LUMO (Supporting Information Fig. S53 and 61) energy-gap by a destabilized HOMO. The same explanation can be given when comparing **[IrLH$_2$]BF$_4$** to **[LHIr]**. Additionally, the band at 346 nm of **[LHIr]** can be assigned to a MLCT from the Ir-centre onto the Trz-backbone (Supporting Information Fig. S55). This transition hints to a somewhat nucleophilic Ir-centre and a quite electrophilic Trz-backbone which could explain the observed tendency of **[LHIr]** and reported compounds[82] to preferably undergo isomerization from the N_{Py}-N_{exo}- to the cationic N_{Py}-N_{Trz}-coordination mode.

For **[IrLHIr]BF$_4$** two low energy bands at 466 nm and 404 nm were observed which can be assigned to a LMCT from N_{exo} to the coordinatively unsaturated Ir-atom and MMCT from the Cl-bound Ir-atom to the coordinatively unsaturated Ir-atom (Supporting Information Fig. S57)). Upon coordination with PPh_3 (**[IrLHIrPPh$_3$]BF$_4$**), which is connected to a color change from green to yellow, both bands collapse into one band at 424 nm. This band can be assigned to a HOMO-LUMO transition (Supporting Information Fig. S59)). The HOMO of **[IrLHIrPPh$_3$]BF$_4$** is localized on N_{exo}, the Trz-ring and the PPh_3-coordinated Ir-atom while the LUMO mostly resides on the Py-substituent of the triazole-ligand and the Cl-coordinated Ir-atom. This transition therefore translates to a mixture of a LLCT (Trz + N_{exo} to Py), a LMCT (Trz + N_{exo} to *Ir*-Cl) and a MMCT (*Ir*-PPh_3 to *Ir*-Cl) which is in a complete contrast to the transitions observed for the complex **[IrLHIr]BF$_4$** with a coordinatively unsaturated Ir-atom.

Judging from the absorption spectra and the supporting computational results, the electronic structure of the different herein presented Ir-complexes can be tuned quite easily.

Table 1. Selected crystallographic and spectroscopic data of the herein reported compounds.

Compound	C1-N4 [Å]	N4-R [Å]	C1-N4-R [°]	δ^{1H}(-N*H*) [ppm]
LH$_2$	1.360(2)/1.358(3)[h]	-	-	5.37[a], 4.95[b], 4.95[c]
[LH]$_2$Zn	1.337(5)/1.331(5)[h]	1.924(4)/1.907(4) [h]	119.4(3)/117.8(3) [h]	3.18[b], 3.63[d]
[IrLH$_2$]BF$_4$	1.332(5)	-	-	5.47[d]
[LHIr]	1.317(3)	2.063(2)	123.4(2)	2.64[d]
[L'HIr]BF$_4$	1.309(4)	2.060(3)	123.7(2)	-
^{Ph}LIr(ACN)[m]	1.322(3)	2.096(2)	117.4(2)	4.86[e]
^{Ph}LIr[m]	1.33(1)	1.986(8)	128.8(7)	11.30[l]
[LH$_2$](X)$_2$	1.328(3)[j]	-	-	6.39[e,j], 6.09[e,k]
[LHIr](BF$_4$)$_2$	-	-	-	3.94[e]
IrLH	1.301(5)	-	-	4.81[c], 4.76[f]
IrLRh	1.323(6)	2.075(4)	137.4(4)	3.37[d]
IrLC$_6$F$_5$	1.312(7)	1.346(8)	123.1(5)	-

[IrLHIr]BF$_4$	1.33(1)	1.999(8)	125.4(7)	9.01[d], 7.94[e]
[IrLHIrPPh$_3$]BF$_4$	1.324(7)[i]	2.102(5)[i]	119.5(4)[i]	1.03/0.87[d,g]
[RhLH$_2$]BF$_4$	1.351(2)	-	-	5.34[d], 5.58[e]
[RhLHIr]BF$_4$	1.341(6)	1.996(4)	124.8(4)	9.00[d]
[ReLH$_2$]OTf	1.349(3)	-	-	6.07[d]

[a]: Recorded in $CDCl_3$. [b]: Recorded in C_6D_6. [c]: Recorded in toluene-d8. [d]: Recorded in CD_2Cl_2. [e]: Recorded in CD_3CN. [f]: Recorded in THF-d8. [g]: Diastereomeric mixture of cis- and trans-isomer.[h]: Two independent molecules in the asymmetric unit. [i]: Cis-diastereomer. [j]: X = OTf. [k]: X = BF_4. [l]: Recorded in acetone-d6. [m]: Data taken from ref. 79.

The herein presented route to synthesize metallo-MIIs was transferred to different metals in order to investigate the viability of the chosen route. For this, **LH$_2$** was reacted with either $Re(CO)_5OTf$ or $[RhCp^*Cl_2]_2$ respectively resulting in the triazolium salts **[MLH$_2$]X**, which could be isolated in good yields and characterized by (^{1}H, ^{13}C)-NMR-and IR-spectroscopy (for **[ReLH$_2$]OTf**, Supporting Information Fig. S 48), mass spectrometry, CHN-analysis and sc-XRD (Scheme 9). The deprotonation of both compounds resulted in the formation of solution with intense colors. In the case of **ReLH** the desired MII could not be detected by NMR-spectroscopy or MS-methods. The ^{1}H-NMR-spectrum of the crude reaction mixture shows broad and poorly resolved signals indicating the formation of an oligomer (see SI for details and proposed mechanism). We assume, as also crystallization of the compound was not possible, that the *in situ* formed MII **ReLH** reacts with either a carbonyl-coligand of another molecule of **ReLH** or under ligand-substitution of one CO-coligand by the highly nucleophilic N-atom of the MII-ligand under the formation of a coordination polymer. IR-spectroscopic measurements before and after deprotonation (Supporting Information Fig. S 48) reinforce this hypothesis as after deprotonation only three carbonyl-stretching modes were detected. In the case of **RhLH** work up afforded a brown powder from which no substances could be identified. Following up the deprotonation reaction *via* ^{1}H-NMR-spectroscopy revealed that the deprotonation of **[RhLH$_2$]BF$_4$** is unselective and from the reaction mixture no product could be identified. As with **ReLH**, we assume a tail-biting mechanism of **RhLH** or the *in situ* deprotonation of newly generated Rh-MII (**RhLH**) resulting in a variety of different products (see SI for details). These assumptions are backed up by theoretical calculations, which show that the LUMOs (Figure 1) of **ReLH** (Supporting Information Tbl. S 28) and **RhLH** (Supporting Information Tbl. S 30) are energetically accessible and mostly located on the ML_n fragment (Supporting Information Fig. S 67 and 68). This suggests a very pronounced eletrophilicity of the ML_n fragment compared to **IrLH**, which in contrast to **ReLH** and **RhLH** could be isolated.

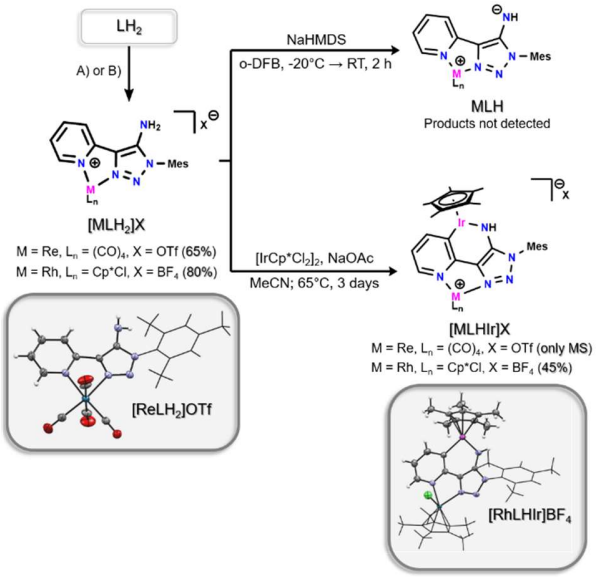

Scheme 9. Synthesis of metallo-MII precursors and reactivity thereof. A) For M = Re: Re(CO)$_5$OTf, DCM, 16 h, RT. B) for M = Rh: 1.) $[RhCp^*Cl_2]_2$, DCM/acetone, 1 h, RT. 2.) NH_4BF_4, DCM/acetone, 1 h, RT. Respective molecular structures are shown in ORTEP-representation in the crystals obtained by sc-XRD. Selected fragments are displayed in wireframe representation. Counter-anions are omitted for clarity.

As the free metallo-MIIs **MLH** were not isolable, we conducted C-H activation reactions of the triazolium salts **[MLH$_2$]X** with the $IrCp^*Cl_2$-Dimer. During this reaction the corresponding metallo-MII is generated *in situ* and directly coordinated thus giving the possibility to catch the corresponding metallo-MIIs indirectly by coordination to IrCp* (**[MLHIr]X**). For the Rh-analogue the corresponding heterodinuclear Rh/Ir-complex **[RhLHIr]BF$_4$** was isolated with a yield of 45%. The product identity was confirmed by elemental analysis, MS, NMR-spectroscopy and sc-XRD. The dark-green color and the highly deshielded signal in the ^{1}H-NMR spectrum (Supporting Information Fig. S45) assigned to –N*H* points to a coordinatively unsaturated Ir-centre which was further confirmed by single-crystal XRD (Scheme 9). This observation follows the trend established for the Ir-analogue **[IrLHIr]BF$_4$** (Scheme 6). **[RhLHIr]BF$_4$** is thus a rare example of a heterodinuclear metal complex with *meta*-C-H activation, and a combination of one coordinatively saturated (Rh) and one coordinatively unsaturated (Ir) metal centers.

The corresponding $Re(CO)_4$-analogue **[ReLHIr]OTf** could be detected by mass-spectrometry while ^{1}H-NMR spectroscopy conducted on the crude material indicated the formation of the desired compound but also revealed the formation of a product mixture.

In summary, we have shown here that 5-amino-4-pyridyl-1,2,3-triazole is a versatile synthon for generating a series of interesting compounds. The first examples of amido-complexes based on a 1,2,3-triazole platform, and the first example of a normal (as opposed to mesoionic) triazole-based imine have been presented here. Most intriguingly, by using metalation of the N-pyridyl/*N*3-triazole chelating pocket (as opposed to alkylation/arylation at the *N*3-triazole), we were able to generate the first examples of metallo-MII. These metallo-MIIs are versatile compounds in which the modularity of the synthesis of aminotriazoles can be combined with the functionality of the metal fragment at the backbone to generate compounds with very interesting properties. The metallo-MIIs are extremely strong donors and at the same time possess accepting properties because of the incorporation of the metal fragments. Such compounds are thus ambivalent and contain both a nucleophilic and an electrophilic center. The metallo-MIIs can engage in strong intramolecular hydrogen bonding, can perform C-F bond activation, as well as *meta*-C-H activation. Additionally, heterodinucelar complexes with a coordinatively saturated and a coordinatively unsaturated metal center can be readily and selectively synthesized based on the metallo-MIIs. In view of the modular synthesis, the easy incorporation of additional functionalities through the metal fragments, the electronic adaptability, and their intriguing bond activation ability, we believe that this new compound class will have a strong impact on synthetic chemistry, catalysis and beyond in the coming years.

ASSOCIATED CONTENT

Supporting Information. Additional information regarding synthetic procedures, spectroscopic/spectrometric data (NMR, UV-vis, IR, MS), crystallographic data and computational details can be found in the Supporting Information. This material is available free of charge via the Internet at http://pubs.acs.org.

CCDC NUmmer:

LH_2 (CCDC #2173943)

$[LH]_2Zn$ (CCDC #2173699)

$[IrLH_2]BF_4$ (CCDC #2283466)

$[LH_2](OTf)_2$ (CCDC #2183155)

[LHIr] (CCDC #2245355)

[L'HIr]BF_4 (CCDC #2245318)

IrLH (CCDC #2323080)

IrLHRh (CCDC #2305937)

$IrLHC_6F_5$ (CCDC #2321172)

[IrLHIr]BF_4 (CCDC #2289129)

[IrLHIrPPh$_3$]BF_4 (CCDC #2312925)

$[RhLH_2]BF_4$ (CCDC #2357574)

[RhLHIr]BF_4 (CCDC #2357970)

$[ReLH_2]OTf$ (CCDC #2324330)

AUTHOR INFORMATION

Corresponding Author

*Biprajit Sarkar –Institut für Anorganische Chemie, Universität Stuttgart, Pfaffenwaldring 55, 70569 Stuttgart, Germany; Email: biprajit.sarkar@iac.uni-stuttgart.de

Author Contributions

RR and BS designed the project. All experiments were carried out by RR. Data interpretation was carried out jointly by both authors. The manuscript was written through contributions of all authors. / All authors have given approval to the final version of the manuscript.

Funding Sources

The present work made use of computational resources supported by the state of Baden-Württemberg through bwHPC and the German Research Foundation (DFG) through grant no. INST 40/575-1 FUGG (JUSTUS 2cluster).

Notes

Any additional relevant notes should be placed here.

ACKNOWLEDGMENT

We want to thank Dr. Falk Lissner, PD Ingo Hartenbach and Dr. Wolfgang Frey for the measurement of X-ray diffraction data. We further want to thank Barbara Förtsch for elemental analyses and the analytical department of the Institute of Organic Chemistry of the University of Stuttgart for recording mass and NMR spectra. Derman Batman is dearly thanked for fruitful discussions on semantics.

ABBREVIATIONS

Py, pyridyl; MIC, mesoionic carbene; NHC, N-heterocyclic carbene; MIO, mesoionic olefin; Cp*, μ^5-(C_5Me_5); MII, mesoionic imine; PDI, pyridinediimine; bpy, 2,2'-bipyridine; 2,2':6'2''-terpyridine; NaOAc, sodium acetate; ORTEP, Oak Ridge Thermal-Ellipsoid Plot; (sc-)XRD, (single-crystal) X-ray diffractometry; HMDS, hexamethyldisilazane; Trz, 1,2,3-triazole; OTf, F_3CSO_3; NMR, nuclear magnetic resonance; ppm, parts per million; o-DFB, *ortho*-difluorobenzene; DCM, dichloromethane; IR, infrared; HOMO, highest occupied molecular orbital; LUMO, lowest unoccupied molecular orbital; FTIR, Fourier-transformed infrared; TEP, Tolmann electronic parameter; SI, supplementary information; Mes, 2,4,6-trimethylphenyl; THF, tetrahydrofurane; UV-vis, ultraviolet and visible light; (TD)-DFT, (time-dependent) density functional theory; LLCT, ligand-to-ligand charge transfer; LMCT, ligand-to-metal charge transfer; MLCT, metal-to-ligand charge transfer; MMCT, metal-to-metal charge transfer; N_{exo}, exocyclic nitrogen atom on MIIs; δ, chemical shift (NMR-spectroscopy); MS, mass-spectrometry; mCPBA. Meta-chloroben-zoic acid.

REFERENCES

(1) Hawecker, J.; Lehn, J.-M.; Ziessel, R. Electrocatalytic reduction of carbon dioxide mediated by Re(bipy)(CO) 3 Cl (bipy = 2,2'-bipyridine). J. Chem. Soc., Chem. Commun. ***1984*** *(6), 328–330. DOI: 10.1039/C39840000328.*

(2) Stein, F.; Nößler, M.; Hazari, A. S.; Böser, L.; Walter, R.; Liu, H.; Klemm, E.; Sarkar, B. Ruthenium Complexes of Polyfluorocarbon Substituted Terpyridine and Mesoionic Carbene Ligands: An Interplay in CO2 Reduction. Eur. J. Chem. ***2023****, 29 (31), e202300405. DOI: 10.1002/chem.202300405. Published Online: Apr. 24, 2023.*

(3) Schubert, U. S.; Hofmeier, H.; Newkome, G. R. Modern Terpyridine Chemistry; Wiley, 2006. DOI: 10.1002/3527608486.

(4) Ryabov, A. D.; Soukharev, V. S.; Alexandrova, L.; Le Lagadec, R.; Pfeffer, M. Low-potential cyclometalated osmium(II) mediators of glucose oxidase. Inorg. Chem. ***2003****, 42 (21), 6598–6600. DOI: 10.1021/ic0346578.*

(5) Bio-Inspired Iron and Nickel Complexes. In Inorganic Syntheses; Rauchfuss, T. B., Ed.; John Wiley & Sons, Inc, 2010; pp 129–147. DOI: 10.1002/9780470651568.ch7.

(6) Gonell, S.; Massey, M. D.; Moseley, I. P.; Schauer, C. K.; Muckerman, J. T.; Miller, A. J. M. The Trans Effect in Electrocatalytic CO2 Reduction: Mechanistic Studies of Asymmetric Ruthenium Pyridyl-Carbene Catalysts. J. Am. Chem. Soc. ***2019****, 141 (16), 6658–6671. DOI: 10.1021/jacs.9b01735. Published Online: Apr. 11, 2019.*

(7) Derrick, J. S.; Loipersberger, M.; Chatterjee, R.; Iovan, D. A.; Smith, P. T.; Chakarawet, K.; Yano, J.; Long, J. R.; Head-Gordon, M.; Chang, C. J. Metal-Ligand Cooperativity via Exchange Coupling Promotes Iron- Catalyzed Electrochemical CO2 Reduction at Low Overpotentials. J. Am. Chem. Soc. ***2020****, 142 (48), 20489–20501. DOI: 10.1021/jacs.0c10664. Published Online: Nov. 18, 2020.*

(8) Gonell, S.; Assaf, E. A.; Duffee, K. D.; Schauer, C. K.; Miller, A. J. M. Kinetics of the Trans Effect in Ruthenium Complexes Provide Insight into the Factors That Control Activity and Stability in CO2 Electroreduction. J. Am. Chem. Soc. ***2020****, 142 (19), 8980–8999. DOI: 10.1021/jacs.0c02912. Published Online: May. 4, 2020.*

(9) Elgrishi, N.; Chambers, M. B.; Artero, V.; Fontecave, M. Terpyridine complexes of first row transition metals and electrochemical reduction of CO_2 to CO. Phys. Chem. Chem. Phys. ***2014****, 16 (27), 13635–13644. DOI: 10.1039/C4CP00451E. Published Online: Mar. 20, 2014.*

(10) Elgrishi, N.; Chambers, M. B.; Fontecave, M. Turning it off! Disfavouring hydrogen evolution to enhance selectivity for CO production during homogeneous CO2 reduction by cobalt-terpyridine complexes. Chem. ***2015****, 6 (4), 2522–2531. DOI: 10.1039/C4SC03766A. Published Online: Feb. 18, 2015.*

(11) Elgrishi, N.; Griveau, S.; Chambers, M. B.; Bedioui, F.; Fontecave, M. Versatile functionalization of carbon electrodes with a polypyridine ligand: metallation and electrocatalytic H(+) and CO2 reduction. Chem Commun (Camb) ***2015****, 51 (14), 2995–2998. DOI: 10.1039/C4CC10027A.*

(12) Hartshorn, C. M.; Maxwell, K. A.; White, P. S.; DeSimone, J. M.; Meyer, T. J. Separation of positional isomers of oxidation catalyst precursors. Inorg. Chem. ***2001****, 40 (4), 601–606. DOI: 10.1021/ic9911724.*

(13) Esswein, A. J.; Nocera, D. G. Hydrogen production by molecular photocatalysis. Chem. Rev. ***2007****, 107 (10), 4022–4047. DOI: 10.1021/cr050193e.*

(14) Guillemard, L.; Wencel-Delord, J. When metal-catalyzed C-H functionalization meets visible-light photocatalysis. Beilstein J. Org. Chem. ***2020****, 16 (1), 1754–1804. DOI: 10.3762/bjoc.16.147. Published Online: Jul. 21, 2020.*

(15) Camara, F.; Gavaggio, T.; Dautreppe, B.; Chauvin, J.; Pécaut, J.; Aldakov, D.; Collomb, M.-N.; Fortage, J. Electrochemical Properties of a Rhodium(III) Mono-Terpyridyl Complex and Use as a Catalyst for Light-Driven Hydrogen Evolution in Water. Molecules ***2022****, 27 (19), 6614. DOI: 10.3390/molecules27196614. Published Online: Oct. 5, 2022.*

(16) Schott, O.; Pal, A. K.; Chartrand, D.; Hanan, G. S. A Bisamide Ruthenium Polypyridyl Complex as a Robust and Efficient Photosensitizer for Hydrogen Production. ChemSusChem ***2017****, 10 (22), 4436–4441. DOI: 10.1002/cssc.201701543. Published Online: Oct. 16, 2017.*

(17) Schultz, D. M.; Yoon, T. P. Solar synthesis: prospects in visible light photocatalysis. Science ***2014****, 343 (6174), 1239176. DOI: 10.1126/science.1239176.*

(18) Shon, J.-H.; Teets, T. S. Photocatalysis with Transition Metal Based Photosensitizers. Comments Inorg. Chem. ***2020****, 40 (2), 53–85. DOI: 10.1080/02603594.2019.1694517.*

(19) Förster, C.; Heinze, K. Photophysics and photochemistry with Earth-abundant metals - fundamentals and concepts. Chem. Soc. Rev. ***2020****, 49 (4), 1057–1070. DOI: 10.1039/C9CS00573K.*

(20) Förster, C.; Heinze, K. Bimolecular reactivity of 3d metal-centered excited states (Cr, Mn, Fe, Co). Chem. Phys. Rev. ***2022****, 3 (4). DOI: 10.1063/5.0112531.*

(21) Treiling, S.; Wang, C.; Förster, C.; Reichenauer, F.; Kalmbach, J.; Boden, P.; Harris, J. P.; Carrella, L. M.; Rentschler, E.; Resch-Genger, U.; Reber, C.; Seitz, M.; Gerhards, M.; Heinze, K. Luminescence and Light-Driven Energy and Electron Transfer from an Exceptionally Long-Lived Excited State of a Non-Innocent Chromium(III) Complex. Angew. Chem. Int. Ed. ***2019****, 58 (50), 18075–18085. DOI: 10.1002/anie.201909325. Published Online: Oct. 31, 2019.*

(22) Wegeberg, C.; Wenger, O. S. Luminescent First-Row Transition Metal Complexes. JACS Au ***2021****, 1 (11), 1860–1876. DOI: 10.1021/jacsau.1c00353. Published Online: Sep. 24, 2021.*

(23) Nößler, M.; Neuman, N. I.; Böser, L.; Jäger, R.; Singha Hazari, A.; Hunger, D.; Pan, Y.; Lücke, C.; Bens, T.; van Slageren, J.; Sarkar, B. Spin Crossover and Fluorine-Specific Interactions in Metal Complexes of Terpyridines with Polyfluorocarbon Tails. Chem. Eur. J. ***2023****, 29 (46), e202301246. DOI: 10.1002/chem.202301246. Published Online: Jul. 6, 2023.*

(24) Nößler, M.; Jäger, R.; Hunger, D.; Reimann, M.; Bens, T.; Neuman, N. I.; Singha Hazari, A.; Kaupp, M.; van Slageren, J.; Sarkar, B. Electrochemistry and Spin-Crossover Behavior of Fluorinated Terpyridine-Based Co(II) and Fe(II) Complexes. Eur. J. Inorg. Chem. ***2023****, 26 (19), e202300091. DOI: 10.1002/ejic.202300091.*

(25) Gütlich, P.; Goodwin, H. A. Spin crossover in transition metal compounds; Topics in current chemistry, Vol. 234; Springer, 2004. DOI: 10.1007/b93641.

(26) Sato, O. Dynamic molecular crystals with switchable physical properties. Nature Chem ***2016****, 8 (7), 644–656. DOI: 10.1038/nchem.2547.*

(27) Senthil Kumar, K.; Ruben, M. Emerging trends in spin crossover (SCO) based functional materials and devices. Coord. Chem. Rev. ***2017****, 346, 176–205. DOI: 10.1016/j.ccr.2017.03.024.*

(28) Nakanishi, T.; Hori, Y.; Wu, S.; Sato, H.; Okazawa, A.; Kojima, N.; Horie, Y.; Okajima, H.; Sakamoto, A.; Shiota, Y.; Yoshizawa, K.; Sato, O. Three-Step Spin State Transition and Hysteretic Proton Transfer in the Crystal of an Iron(II) Hydrazone Complex. Angew. Chem. Int. Ed. ***2020****, 59 (35), 14781–14787. DOI: 10.1002/anie.202006763. Published Online: Jul. 13, 2020.*

(29) Winter, A.; Schubert, U. S. Metal-Terpyridine Complexes in Catalytic Application – A Spotlight on the Last Decade. ChemCatChem ***2020****, 12 (11), 2890–2941. DOI: 10.1002/cctc.201902290.*

(30) Zafar, M. N.; Atif, A. H.; Nazar, M. F.; Sumrra, S. H.; Gul-E-Saba; Paracha, R. Pyridine and related ligands in transition metal homogeneous catalysis. Russ J Coord Chem ***2016****, 42 (1), 1–18. DOI: 10.1134/S1070328416010097.*

(31) Wachenfeldt, H. von; Polukeev, A. V.; Loganathan, N.; Paulsen, F.; Röse, P.; Garreau, M.; Wendt, O. F.; Strand, D. Cyclometallated gold(III) aryl-pyridine complexes as efficient catalysts for three-component synthesis of substituted oxazoles. Dalton Trans. ***2015****, 44 (12), 5347–5353. DOI: 10.1039/C4DT03806A.*

(32) Knijnenburg, Q.; Horton, A. D.; van der Heijden, H.; Kooistra, T. M.; Hetterscheid, D. G.; Smits, J. M.; Bruin, B. de; Budzelaar, P. H.; Gal, A. W. Olefin hydrogenation using diimine pyridine complexes of Co and Rh. J. Mol. Catal. A Chem. ***2005****, 232 (1-2), 151–159. DOI: 10.1016/j.molcata.2004.12.039.*

(33) Chirik, P. J. Iron- and Cobalt-Catalyzed Alkene Hydrogenation: Catalysis with Both Redox-Active and Strong Field Ligands. Acc. Chem. Res. ***2015****, 48 (6), 1687–1695. DOI: 10.1021/acs.accounts.5b00134. Published Online: Jun. 4, 2015.*

(34) Joannou, M. V.; Bezdek, M. J.; Chirik, P. J. Pyridine(diimine) Molybdenum-Catalyzed Hydrogenation of Arenes and Hindered Olefins: Insights into Precatalyst Activation and Deactivation Pathways. ACS Catal. ***2018****, 8 (6), 5276–5285. DOI: 10.1021/acscatal.8b00924.*

(35) Schuster, C. H.; Diao, T.; Pappas, I.; Chirik, P. J. Bench-Stable, Substrate-Activated Cobalt Carboxylate Pre-Catalysts for Alkene Hydrosilylation with Tertiary Silanes. ACS Catal. **2016**, 6 (4), 2632–2636. DOI: 10.1021/acscatal.6b00304.

(36) Zhou, S.; Chen, C. Synthesis of silicon-functionalized polyolefins by subsequent cobalt-catalyzed dehydrogenative silylation and nickel-catalyzed copolymerization. Sci. Bull. **2018**, 63 (7), 441–445. DOI: 10.1016/j.scib.2018.02.021. Published Online: Mar. 10, 2018.

(37) De, S.; Kumar S K, A.; Shah, S. K.; Kazi, S.; Sarkar, N.; Banerjee, S.; Dey, S. Pyridine: the scaffolds with significant clinical diversity. RSC Advances **2022**, 12 (24), 15385–15406. DOI: 10.1039/D2RA01571D. Published Online: May. 20, 2022.

(38) Zhao, Q.; Meng, G.; Nolan, S. P.; Szostak, M. N-Heterocyclic Carbene Complexes in C-H Activation Reactions. Chem. Rev. **2020**, 120 (4), 1981–2048. DOI: 10.1021/acs.chemrev.9b00634. Published Online: Jan. 22, 2020.

(39) Nesterov, V.; Reiter, D.; Bag, P.; Frisch, P.; Holzner, R.; Porzelt, A.; Inoue, S. NHCs in Main Group Chemistry. Chem. Rev. **2018**, 118 (19), 9678–9842. DOI: 10.1021/acs.chemrev.8b00079. Published Online: Jul. 3, 2018.

(40) Scott, N. M.; Nolan, S. P. Stabilization of Organometallic Species Achieved by the Use of N-Heterocyclic Carbene (NHC) Ligands. Eur. J. Inorg. Chem. **2005**, 2005 (10), 1815–1828. DOI: 10.1002/ejic.200500030.

(41) Herrmann, W. A. N-Heterocyclic Carbenes: A New Concept in Organometallic Catalysis. Angew. Chem. Int. Ed. **2002**, 41 (8), 1290–1309. DOI: 10.1002/1521-3773(20020415)41:8<1290:AID-ANIE1290>3.0.CO;2-Y.

(42) Frémont, P. de; Marion, N.; Nolan, S. P. Carbenes: Synthesis, properties, and organometallic chemistry. Coord. Chem. Rev. **2009**, 253 (7-8), 862–892. DOI: 10.1016/j.ccr.2008.05.018.

(43) Huynh, H. V. The Organometallic Chemistry of N-heterocyclic Carbenes; John Wiley & Sons, Ltd, 2017. DOI: 10.1002/9781118698785.

(44) Nair, V.; Bindu, S.; Sreekumar, V. N-heterocyclic carbenes: reagents, not just ligands! Angew. Chem. Int. Ed. **2004**, 43 (39), 5130–5135. DOI: 10.1002/anie.200301714.

(45) Maity, R.; Sarkar, B. Chemistry of Compounds Based on 1,2,3-Triazolylidene-Type Mesoionic Carbenes. JACS Au **2022**, 2 (1), 22–57. DOI: 10.1021/jacsau.1c00338. Published Online: Dec. 15, 2021.

(46) Albrecht, M. Chapter Two - Normal and Abnormal N-Heterocyclic Carbene Ligands: Similarities and Differences of Mesoionic C–Donor Complexes. In Advances in Organometallic Chemistry; Pérez, P. J., Ed.; Academic Press, 2014; pp 111–158. DOI: 10.1016/B978-0-12-800976-5.00002-3.

(47) Guisado-Barrios, G.; Soleilhavoup, M.; Bertrand, G. 1H-1,2,3-Triazol-5-ylidenes: Readily Available Mesoionic Carbenes. Acc. Chem. Res. **2018**, 51 (12), 3236–3244. DOI: 10.1021/acs.accounts.8b00480.

(48) Beerhues, J.; Aberhan, H.; Streit, T.-N.; Sarkar, B. Probing Electronic Properties of Triazolylidenes through Mesoionic Selones, Triazolium Salts, and Ir-Carbonyl-Triazolylidene Complexes. Organometallics **2020**, 39 (24), 4557–4564. DOI: 10.1021/acs.organomet.0c00614.

(49) Suntrup, L.; Klenk, S.; Klein, J.; Sobottka, S.; Sarkar, B. Gauging Donor/Acceptor Properties and Redox Stability of Chelating Click-Derived Triazoles and Triazolylidenes: A Case Study with Rhenium(I) Complexes. Inorg. Chem. **2017**, 56 (10), 5771–5783. DOI: 10.1021/acs.inorgchem.7b00393. Published Online: Apr. 21, 2017.

(50) Chassaing, S.; Bénéteau, V.; Pale, P. When CuAAC 'Click Chemistry' goes heterogeneous. Catal. Sci. Technol. **2016**, 6 (4), 923–957. DOI: 10.1039/C5CY01847A.

(51) Hou, J.; Liu, X.; Shen, J.; Zhao, G.; Wang, P. G. The impact of click chemistry in medicinal chemistry. Expert Opin. Drug Discov. **2012**, 7 (6), 489–501. DOI: 10.1517/17460441.2012.682725. Published Online: May. 19, 2012.

(52) Kolb, H. C.; Sharpless, K. B. The growing impact of click chemistry on drug discovery. Drug Discov. Today **2003**, 8 (24), 1128–1137. DOI: 10.1016/S1359-6446(03)02933-7.

(53) Kolb, H. C.; Finn, M. G.; Sharpless, K. B. Click Chemistry: Diverse Chemical Function from a Few Good Reactions. Angew. Chem. Int. Ed. **2001**, 40 (11), 2004–2021. DOI: 10.1002/1521-3773(20010601)40:11<2004:AID-ANIE2004>3.0.CO;2-5.

(54) Hawker, C. J.; Fokin, V. V.; Finn, M. G.; Sharpless, K. B. Bringing Efficiency to Materials Synthesis: The Philosophy of Click Chemistry. Aust. J. Chem. **2007**, 60 (6), 381. DOI: 10.1071/CH07107.

(55) Chang, P. V.; Prescher, J. A.; Sletten, E. M.; Baskin, J. M.; Miller, I. A.; Agard, N. J.; Lo, A.; Bertozzi, C. R. Copper-free click chemistry in living animals. PNAS **2010**, 107 (5), 1821–1826. DOI: 10.1073/pnas.0911116107. Published Online: Jan. 14, 2010.

(56) Meldal, M.; Tornøe, C. W. Cu-catalyzed azide-alkyne cycloaddition. Chem. Rev. **2008**, 108 (8), 2952–3015. DOI: 10.1021/cr0783479.

(57) Bens, T.; Marhöfer, D.; Boden, P.; Steiger, S. T.; Suntrup, L.; Niedner-Schatteburg, G.; Sarkar, B. A Different Perspective on Tuning the Photophysical and Photochemical Properties: The Influence of Constitutional Isomers in Group 6 Carbonyl Complexes with Pyridyl-Mesoionic Carbenes. Inorg. Chem. **2023.** DOI: 10.1021/acs.inorgchem.3c02478. Published Online: Sep. 18, 2023.

(58) Suntrup, L.; Stein, F.; Hermann, G.; Kleoff, M.; Kuss-Petermann, M.; Klein, J.; Wenger, O. S.; Tremblay, J. C.; Sarkar, B. Influence of Mesoionic Carbenes on Electro- and Photoactive Ru and Os Complexes: A Combined (Spectro-)Electrochemical, Photochemical, and Computational Study. Inorg. Chem. **2018**, 57 (21), 13973–13984. DOI: 10.1021/acs.inorgchem.8b02551. Published Online: Oct. 25, 2018.

(59) Klein, J.; Stuckmann, A.; Sobottka, S.; Suntrup, L.; van der Meer, M.; Hommes, P.; Reissig, H.-U.; Sarkar, B. Ruthenium Complexes with Strongly Electron-Donating Terpyridine Ligands: Effect of the Working Electrode on Electrochemical and Spectroelectrochemical Properties. Chem. Eur. J. **2017**, 23 (50), 12314–12325. DOI: 10.1002/chem.201701431. Published Online: Jun. 20, 2017.

(60) Bens, T.; Boden, P.; Di Martino-Fumo, P.; Beerhues, J.; Albold, U.; Sobottka, S.; Neuman, N. I.; Gerhards, M.; Sarkar, B. Chromium(0) and Molydenum(0) Complexes with a Pyridyl-Mesoionic Carbene Ligand: Structural, (Spectro)electrochemical, Photochemical, and Theoretical Investigations. Inorg. Chem. **2020**, 59 (20), 15504–15513. DOI: 10.1021/acs.inorgchem.0c02537. Published Online: Oct. 6, 2020.

(61) Bens, T.; Kübler, J. A.; Walter, R. R. M.; Beerhues, J.; Wenger, O. S.; Sarkar, B. Impact of Bidentate Pyridyl-Mesoionic Carbene Ligands: Structural, (Spectro)Electrochemical, Photophysical, and Theoretical Investigations on Ruthenium(II) Complexes. ACS Org. Inorg. Au **2023**, 3 (4), 184–198. DOI: 10.1021/acsorginorgau.3c00005. Published Online: May. 3, 2023.

(62) Boden, P.; Di Martino-Fumo, P.; Bens, T.; Steiger, S.; Albold, U.; Niedner-Schatteburg, G.; Gerhards, M.; Sarkar, B. NIR-Emissive Chromium(0), Molybdenum(0), and Tungsten(0) Complexes in the Solid State at Room Temperature. Chem. Eur. J. **2021**, 27 (51), 12959–12964. DOI: 10.1002/chem.202102208. Published Online: Aug. 4, 2021.

(63) Bens, T.; Walter, R. R. M.; Beerhues, J.; Schmitt, M.; Krossing, I.; Sarkar, B. The Best of Both Worlds: Combining the Power of MICs and WCAs To Generate Stable and Crystalline CrI -Tetracarbonyl Complexes with π-Accepting Ligands. Chem. Eur. J. **2023**, 29 (50), e202301205. DOI: 10.1002/chem.202301205. Published Online: Jul. 17, 2023.

(64) Leigh, V.; Ghattas, W.; Lalrempuia, R.; Müller-Bunz, H.; Pryce, M. T.; Albrecht, M. Synthesis, Photo-, and Electrochemistry of Ruthenium Bis(bipyridine) Complexes Comprising a N- heterocyclic Carbene Ligand. Inorg. Chem. **2013**, 52 (9), 5395–5402. DOI: 10.1021/ic400347r.

(65) Bernet, L.; Lalrempuia, R.; Ghattas, W.; Mueller-Bunz, H.; Vigara, L.; Llobet, A.; Albrecht, M. Tunable single-site ruthenium catalysts for efficient water oxidation. Chem Commun (Camb) **2011**, 47 (28), 8058–8060. DOI: 10.1039/C1CC12615F. Published Online: Jun. 16, 2011.

(66) Bolje, A.; Hohloch, S.; Urankar, D.; Pevec, A.; Gazvoda, M.; Sarkar, B.; Košmrlj, J. Exploring the Scope of Pyridyl- and Picolyl-Functionalized 1,2,3-Triazol-5-ylidenes in Bidentate Coordination to Ruthenium(II) Cymene Chloride Complexes. Organometallics **2014**, 33 (10), 2588–2598. DOI: 10.1021/om500287t.

(67) Suntrup, L.; Stein, F.; Klein, J.; Wilting, A.; Parlane, F. G. L.; Brown, C. M.; Fiedler, J.; Berlinguette, C. P.; Siewert, I.; Sarkar, B. Rhenium Complexes of Pyridyl-Mesoionic Carbenes: Photochemical Properties and Electrocatalytic CO2 Reduction. Inorg. Chem. ***2020****, 59 (7), 4215–4227. DOI: 10.1021/acs.inorgchem.9b02591. Published Online: Mar. 10, 2020.*

(68) Kralj, J.; Bolje, A.; Polančec, D. S.; Steiner, I.; Gržan, T.; Tupek, A.; Stojanović, N.; Hohloch, S.; Urankar, D.; Osmak, M.; Sarkar, B.; Brozovic, A.; Košmrlj, J. Half-Sandwich Ir(III) and Os(II) Complexes of Pyridyl-Mesoionic Carbenes as Potential Anticancer Agents. Organometallics ***2019****, 38 (21), 4082–4092. DOI: 10.1021/acs.organomet.9b00327.*

(69) Boden, P. J.; Di Martino-Fumo, P.; Bens, T.; Steiger, S. T.; Marhöfer, D.; Niedner-Schatteburg, G.; Sarkar, B. Mechanistic and Kinetic Investigations of ON/OFF (Photo)Switchable Binding of Carbon Monoxide by Chromium(0), Molybdenum(0) and Tungsten(0) Carbonyl Complexes with a Pyridyl-Mesoionic Carbene Ligand. Chem. Eur. J. ***2022****, 28 (51), e202201038. DOI: 10.1002/chem.202201038. Published Online: Jul. 13, 2022.*

*(70) Bens, T.; Walter, R. R. M.; Beerhues, J.; Lücke, C.; Gabler, J.; Sarkar, B. Isolation, Characterization and Reactivity of Key Intermediates Relevant to Reductive (Electro)catalysis with Cp*Rh Complexes containing Pyridyl-MIC (MIC = Mesoionic Carbene) Ligands. Chem. Eur. J.* ***2023****, e202302354. DOI: 10.1002/chem.202302354. Published Online: Sep. 28, 2023.*

(71) Antoni, P. W.; Golz, C.; Holstein, J. J.; Pantazis, D. A.; Hansmann, M. M. Isolation and reactivity of an elusive diazoalkene. Nat. Chem. ***2021****, 13 (6), 587–593. DOI: 10.1038/s41557-021-00675-5.*

(72) Antoni, P. W.; Reitz, J.; Hansmann, M. M. N2/CO Exchange at a Vinylidene Carbon Center: Stable Alkylidene Ketenes and Alkylidene Thioketenes from 1,2,3-Triazole Derived Diazoalkenes. J. Am. Chem. Soc. ***2021****, 143 (32), 12878–12885. DOI: 10.1021/jacs.1c06906.*

(73) Liang, Q.; Hayashi, K.; Zeng, Y.; Jimenez-Santiago, J. L.; Song, D. Constructing fused N-heterocycles from unprotected mesoionic N-heterocyclic olefins and organic azides via diazo transfer. Chem Commun (Camb) ***2021****, 57 (50), 6137–6140. DOI: 10.1039/D1CC02245H.*

(74) Zhang, Z.; Huang, S.; Huang, L.; Xu, X.; Zhao, H.; Yan, X. Synthesis of Mesoionic N-Heterocyclic Olefins and Catalytic Application for Hydroboration Reactions. J. Org. Chem. ***2020****, 85 (19), 12036–12043. DOI: 10.1021/acs.joc.0c00257. Published Online: Sep. 23, 2020.*

(75) Kase, D.; Haraguchi, R. Fluoride-Mediated Nucleophilic Aromatic Amination of Chloro-1H-1,2,3-triazolium Salts. Org. Lett. ***2021.*** *DOI: 10.1021/acs.orglett.1c03677. Published Online: Dec. 16, 2021.*

(76) Kase, D.; Takada, T.; Tsuji, N.; Mitsuhashi, T.; Haraguchi, R. Synthesis and Application of Amino-1 H -1,2,3-triazolium Salts. Asian J. Org. Chem. ***2023****, 12 (6), e202300108. DOI: 10.1002/ajoc.202300108.*

(77) Huang, S.; Wu, Y.; Huang, L.; Hu, C.; Yan, X. Synthesis, Characterization and Photophysical Properties of Mesoionic N-Heterocyclic Imines. Chem. Asian J. ***2022.*** *DOI: 10.1002/asia.202200281. Published Online: May. 2, 2022.*

(78) Hansmann, M. M.; Antoni, P. W.; Pesch, H. Stable Mesoionic N-Heterocyclic Olefins (mNHOs). Angew. Chem. Int. Ed. ***2020****, 59 (14), 5782–5787. DOI: 10.1002/anie.201914571.*

(79) Rudolf, R.; Neuman, N. I.; Walter, R. R. M.; Ringenberg, M. R.; Sarkar, B. Mesoionic Imines (MIIs): Strong Donors and Versatile Ligands for Transition Metals and Main Group Substrates. Angew. Chem. Int. Ed. ***2022****, 61 (25), e202200653. DOI: 10.1002/anie.202200653. Published Online: Apr. 19, 2022.*

(80) Rudolf, R.; Batman, D.; Mehner, N.; Walter, R. R. M.; Sarkar, B. Redox-Active Triazole-Derived Mesoionic Imines with Ferrocenyl Substituents and their Metal Complexes: Directed Hydrogen-Bonding, Unusual C-H Activation and Ion-Pair Formation. Chem. Eur. J. ***2024****, e202400730. DOI: 10.1002/chem.202400730. Published Online: Apr. 18, 2024.*

(81) Schweinfurth, D.; Hettmanczyk, L.; Suntrup, L.; Sarkar, B. Metal Complexes of Click-Derived Triazoles and Mesoionic Carbenes: Electron Transfer, Photochemistry, Magnetic Bistability, and Catalysis. ZAAC ***2017****, 643 (9), 554–584. DOI: 10.1002/zaac.201700030.*

(82) Liu, S.; Müller, P.; Takase, M. K.; Swager, T. M. "Click" synthesis of heteroleptic tris-cyclometalated iridium(III) complexes: Cu(I) triazolide intermediates as transmetalating reagents. Inorg. Chem. ***2011****, 50 (16), 7598–7609. DOI: 10.1021/ic2005985. Published Online: Jul. 13, 2011.*

(83) Huynh, H. V. Electronic Properties of N-Heterocyclic Carbenes and Their Experimental Determination. Chem. Rev. ***2018****, 118 (19), 9457–9492. DOI: 10.1021/acs.chemrev.8b00067.*

(84) Anga, S.; Chandra, S.; Sarkar, P.; Das, S.; Mandal, D.; Kundu, A.; Rawat, H.; Schulzke, C.; Sarkar, B.; Pati, S. K.; Chandrasekhar, V.; Jana, A. Facile One-Pot Assembly of Push–Pull Imines by a Selective C–F Substitution Process in Aryl Fluorides. EurJOC ***2020****, 2020 (48), 7445–7449. DOI: 10.1002/ejoc.202001344.*

(85) Mandal, D.; Chandra, S.; Neuman, N. I.; Mahata, A.; Sarkar, A.; Kundu, A.; Anga, S.; Rawat, H.; Schulzke, C.; Mote, K. R.; Sarkar, B.; Chandrasekhar, V.; Jana, A. Activation of Aromatic C−F Bonds by a N-Heterocyclic Olefin (NHO). Chem. Eur. J. ***2020****, 26 (27), 5951–5955. DOI: 10.1002/chem.202000276.*

(86) Pait, M.; Kundu, G.; Tothadi, S.; Karak, S.; Jain, S.; Vanka, K.; Sen, S. S. C−F Bond Activation by a Saturated N-Heterocyclic Carbene: Mesoionic Compound Formation and Adduct Formation with B(C 6 F 5) 3. Angew. Chem. ***2019****, 131 (9), 2830–2834. DOI: 10.1002/ange.201814616.*

(87) Ališ, B.; Tavčar, G. Reaction of N-heterocyclic carbene (NHC) with different HF sources and ratios – A free fluoride reagent based on imidazolium fluoride. J. Fluor. Chem. ***2016****, 192, 141–146. DOI: 10.1016/j.jfluchem.2016.11.004.*

.